Stress-Dependent Electrical Contact Resistance at Fractal Rough Surfaces

Chongpu Zhai[1]; Dorian Hanaor[2]; Gwénaëlle Proust[3]; and Yixiang Gan[4]

Abstract: The electrical contact resistance between contacting rough surfaces was studied under various compressive stresses. The samples considered here were isotropically roughened aluminium disks with upper and lower surfaces modified through polishing and sand blasting using different sized glass beads. Fractal geometry and roughness descriptors, including root mean square values of roughness and slope, were used to describe the topography of sample surfaces, based on the digitized profiles obtained from interferometry-based profilometry. The electrical contact resistances at the interfaces were obtained by applying a controlled current and measuring the resulting voltage, through the following scenarios: (1) over time for various applied testing currents, the resistance relaxation curves were measured at constant loads; (2) through voltage-current characteristics by means of a logarithmic sweeping current, the influence of the testing current on the electrical response of contacting rough surfaces was evaluated; and (3) for a given testing current, the electrical resistance through interfaces of different surface structures was measured under increasing compressive stresses. The experimental results show that the measured resistance depends closely on the measurement time, testing current, surface topology, and mechanical loading. At stresses from 0.03 to 1.18 MPa, the electrical resistance as a function of applied normal stress is found to follow a power law relation, the exponent of which is closely linked to the surface topology. **DOI:** 10.1061/(ASCE)EM.1943-7889.0000967. *© 2015 American Society of Civil Engineers.*

Author keywords: Rough surfaces; Electrical contact resistance; Branly effect; Fractal dimension.

Introduction

The properties of the electrical contact resistance (ECR) at electrical connections are of tremendous importance in many engineering applications, including resistance spot welding, diagnostic tribology, signal, and current transmission (Crinon and Evans 1998; Kogut and Komvopoulos 2003; Kogut and Komvopoulos 2005; Slade 2013). For most applications, e.g., electronic connectors (Bryant and Jin 1991), switches, and electrode structures of batteries (Meulenberg et al. 2003), a low and stable contact resistance is sought after. In these situations, numerous factors can affect the current flow through contacting surfaces, e.g., surface topography, environmental conditions, mechanical loads, the presence of a coating layer, and applied voltage. Vibrations, fretting, thermal shock, and chemical contamination are principal failure mechanisms at electrical contacts often resulting in the malfunction of electric circuits. Effective electrical contacts require reliable mechanical contact in order to avoid failure. Surface characteristics, such as roughness, curvature, and fractal dimension, play an important role in facilitating the closing and opening of electric circuits created by the close contact between surfaces (Bryant and Jin 1991; Oh et al. 1999; Kogut and Etsion 2000; Falcon et al. 2004; Kogut 2005).

The true area of contact at an interface is considerably smaller than the apparent or nominal contact area because of the existence of surface roughness (Archard 1957; Bowden and Williamson 1958; Greenwood and Williamson 1958). When two rough surfaces are squeezed together contact is made through individual asperities with contact patches that can extend in size down to the nanoscale. These contact junctions exhibit electrical and mechanical properties that may diverge from bulk properties (Jackson et al. 2012). Current flowing through rough interfaces is scattered across many contacting asperities with electronic transport involving multiple mechanisms, including quantum tunneling (Yanson et al. 1998; Foley et al. 1999; Agraït et al. 2003), Sharvin contact (Sharvin 1965), and Holm contact (Holm and Holm 1967), depending on the size of contacting junctions and the mean free path of electrons. Early work by Holm and Holm (1967) concluded that the ECR is affected by both the constriction resistance resulting from the limited areas of true contact at an interface and interfacial resistance due to the inevitable presence of resistive surface films, such as oxide layers. When two metal surfaces are compressed together with sufficient pressure, surface asperities can penetrate the oxide layer thus forming metal-to-metal contact patches. When the size of contacting asperities becomes larger than the mean free path of electrons, Holm contact will be the dominant transport mechanism, resulting in a relative low resistance. This concept has been further developed by Chang et al. (1987), Ciavarella et al. (2004, 2008), and Jackson et al. (2009). These theoretical and computational studies assumed that individual microcontacts formed by asperities, where the circuit continuity was established, governed specific electron transport regions, limited by the measuring resolution.

The asperities of contacting surfaces tend to exhibit complex geometries and structures at a wide range of length scales, governing physical properties and interfacial phenomena and giving rise to constriction resistance. The fractal topography based on scale-invariant parameters provides an effective means for modeling engineering surfaces with random self-affine multiscale

[1]Ph.D. Candidate, School of Civil Engineering, Univ. of Sydney, Sydney, NSW 2006, Australia. E-mail: czha1730@uni.sydney.edu.au

[2]Research Fellow, School of Civil Engineering, Univ. of Sydney, Sydney, NSW 2006, Australia. E-mail: dorian.hanaor@sydney.edu.au

[3]Senior Lecturer, School of Civil Engineering, Univ. of Sydney, Sydney, NSW 2006, Australia. E-mail: gwenaelle.proust@sydney.edu.au

[4]Lecturer, School of Civil Engineering, Univ. of Sydney, Sydney, NSW 2006, Australia (corresponding author). E-mail: yixiang.gan@sydney.edu.au

properties (Yan and Komvopoulos 1998; Kogut and Komvopoulos 2004). A general ECR theory based on fractal geometry was proposed in order to describe the effects of contact loads, elastic-plastic deformation of the contacting asperities, surface topography, and material properties on size-dependent electrical resistance of the microcontacts comprising the true contact area (Mikrajuddin et al. 1999; Kogut and Komvopoulos 2003). Kogut et al. (2005) further investigated conductive rough surfaces separated by a thin insulating film. Semiempirical power-law type correlations between the contact resistance and the normal pressure have also been proposed. For contacting surfaces separated by superficial oxide or impurity layers, the power law is found, with the exponent value possibly greater than 1 (Milanez et al. 2003; Falcon and Castaing 2005; Paggi and Barber 2011). The power-law relation between the applied normal load and the contact conductance at rough surfaces has been reported on the basis of the incremental stiffness, which was found to be linearly proportional to the contact conductance (Barber 2003; Pohrt and Popov 2012; Pohrt and Popov 2013; Hanoar et al. 2015).

Furthermore, the influencing factors of ECR include the physical and chemical origins and details of the oxidation processes in corrosive environment (Sun et al. 1999; Sun 2001), surface diffusion (Crinon and Evans 1998; Ogumi and Inaba 1998) and fretting corrosion (Bryant 1994). Thin oxide or hydroxide layers, acting as resistive films with typical thickness ranging from 1 to 10 nm, tend to form at metallic surfaces, covering the contacting surface, and increasing the contact resistance (Bryant and Jin 1991). In conduction through interfaces, insulating layers can bring about high electrical resistance under conditions of low current. With an increasing current this high initial resistance decreases by several orders of magnitude showing nonlinear conductivity phenomena, which is called the Coherer effect or Branly effect. The process is featured by voltage creep, hysteresis loops, and voltage saturation effects (Castaing and Laroche 2004; Falcon and Castaing 2005; Bourbatache et al. 2012; Tekaya et al. 2012). Many mechanisms of resistance modification have been reported in conduction phenomena through rough interfaces, including electron tunneling through oxide layers and voids (Creyssels et al. 2007), dielectric breakdown of oxide layers (Dorbolo et al. 2002), localized current-induced welding (Falcon and Castaing 1993), percolation collective process (Falcon and Castaing 2005), and chemical disorder arising with random composition (Creyssels et al. 2009).

Despite recent progress of nanoscale testing technology and surface morphology characterization, a stress-dependence of electrical conduction behavior through rough interfaces with random multiscale texture remains largely unknown. Particularly, existing experimental results are limited. In this paper, the measured ECR of aluminium disk stacks loaded in compression is presented. The surfaces of the disks were modified by polishing and sand blasting in order to obtain a range of rough surfaces. Compressive loads, testing current, and time were varied to study their influence on the ECR.

Sample Preparation and Surface Characterization

In this paper, round disks, with a diameter of 25 mm, made of aluminium alloy were used as specimens. Surfaces were polished followed by sand abrasive blasting processes using different sized particles to modify the surface details and structures at various scales (Hanaor et al. 2013). For each individual sample, both top and bottom were equally treated through standard polishing and sand blasting procedures. The average diameters of the two selected groups of glass beads used in blasting treatments were 50 and 300 μm. Fig. 1 shows scanning electron microscope (SEM) images of the different surface types used in this work. Samples that have been blasted using glass beads of 50 μm are found to exhibit the most complex and roughest surface texture. The treated aluminium surfaces were scanned using an optical surface profilometer (NanoMap 1000WLI, AEP Technology, California) to obtain three-dimensional digitized topographies. Subsequently, RMS roughness, RMS slopes, and fractal dimension were utilized to characterize and compare the surface geometries.

As shown in Table 1, three types of samples with distinct surface details were prepared and characterized prior to electrical testing, with S1, S2, and S3 representing the polished samples, samples blasted using 300 μm diameter glass beads, and samples blasted using 50 μm diameter glass beads, respectively. Before the standard sand blasting treatment, all the sample surfaces were polished and prepared using several polishing steps with the final step using 1 μm diamond suspension. Then, the processed samples were properly cleaned by water and compressed air to remove any embedded glass beads. Cleaning with ethanol and heat treatment (from 110 to 120°C) were also applied to remove surface contamination and moisture. For each surface, the mean values of roughness descriptors with standard deviations over ten 1×1 mm scans from different samples are shown in Table 1. The scaled triangulation method (Dubuc et al. 1989; De Santis et al. 1997; Zahn and Zösch 1999) was used for the calculation of fractal dimension values. A power law relationship is found between the calculated surface area and the length resolution of digitized scan of all the surfaces, exhibiting self-affinity over a range of length scales (from 1 to 100 μm).
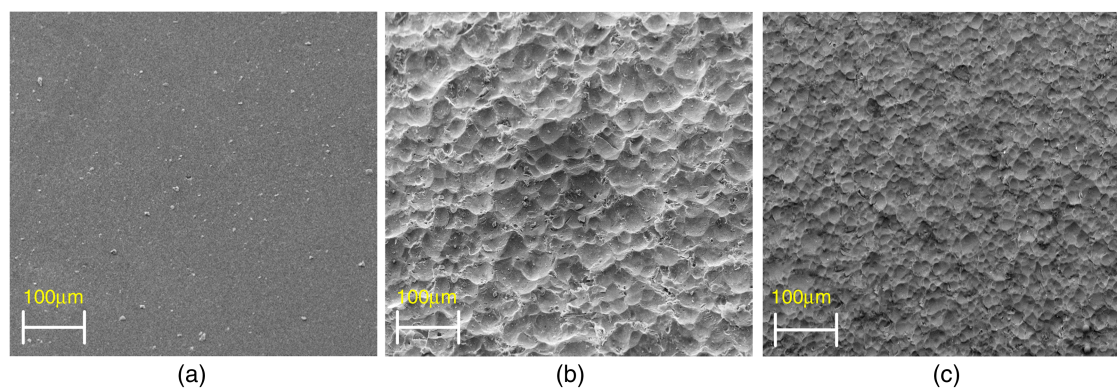

Fig. 1. SEM images of aluminium samples with different surface treatments: (a) polishing treatment; (b) blasted with 300 μm diameter glass beads; (c) blasted with 50 μm diameter glass beads

Table 1. Sample Surface Characterization with Different Treatments

Sample type	Surface treatment	RMS roughness R_{RMS}/μm	RMS slope R_S	Fractal dimension D_f/triangulation
S1	Polished	0.057 ± 0.005	0.009 ± 0.001	2.093 ± 0.0620
S2	Blasted by glass beads of 300 μm diameter	4.179 ± 0.194	0.224 ± 0.015	2.551 ± 0.0217
S3	Blasted by glass beads of 50 μm diameter	2.970 ± 0.276	0.202 ± 0.010	2.626 ± 0.0174

Surfaces blasted with glass beads of 300 μm diameter reveal the highest RMS slope and RMS roughness. The lowest values of RMS roughness, RMS slope and fractal dimension are found for the polished surfaces. The values of lower-roll-off wavelength in the power spectrum of all of the surfaces used were found to be ~100 μm, which is remarkably smaller than the disk diameter (25 mm).

Results and Discussion

Experimental Setup

For each type of sample with similar surface characteristics, electrical resistances were measured for stacks of 11 samples, giving 10 rough to rough interfaces, by means of a source/measurement unit (Agilent B2902A, Keysight Technologies), under various compressive loading forces, as shown in Fig. 2. In this experimental setting, the resistance formed by 10 specimen interfaces placed between two polished plates of the same material instead of one single interface is measured, aiming to achieve a higher precision, larger linear range, and better robustness against measurement noises from the connecting wires, loading device, and measurement unit. A stack of samples can also diminish effectively the experimental errors from the variation of samples with the same surface treatment. Before the experiment, the sample stack was aligned by rotating the top pressure head of the loading machine and using a piece of rubber placed between the pressure head and the top polished plate.

Prior to the measurement of stress-dependent resistance, the following tests were performed: (1) resistance creep tests and (2) sweeping current tests, to exclude the influences from the applied current and measurement time. In the following sections, the results of these tests will be presented and discussed. Finally,

the stress-dependent ECR was measured using the applied current of 10 mA and measuring time of 0.01 s at each individual stress level.

Resistance Creep Tests

The relaxation dynamics of resistance for a given constant current were first investigated to find out the effect of current on the measured resistance over time. The resistance degradation curves at various applied testing currents of 10, 20, 80, 320, and 1,280 mA were recorded, under an applied pressure of 0.061 MPa, as shown in Fig. 3(a). Then, a constant current (320 mA) was applied to study the resistance relaxation under various applied compressive stresses, ranging from 0.031 to 0.490 MPa, as shown in Fig. 3(b). Multiple tests were performed for each individual loading condition, but for clarity here not all the experimental data collected were shown and the trends shown in Fig. 3 are true for all the data collected. The measured resistance under various loads and current conditions gradually decreases with respect to time. For tests carried out under a constant normal load, shown in Fig. 3(a), a higher current brings about a more significant decrease in measured resistance. More specifically, the highest current of 1,280 mA over 200 s was found to cause a decrease of around 15% with reference to the initial measured resistance, whereas a variation of less than 1% was achieved at the lowest current (10 mA). For the tests with the same testing current (320 mA), a higher pressure reduces the trend, which is presented in Fig. 3(b). The measured resistance of the samples under an applied pressure of 0.490 MPa exhibited a slight decrease of less than 2% with reference to the initial resistance, whereas a drop of approximately 15% was found under an applied pressure of 0.031 MPa. For all the tests when the conduction time is less than 1 s, the decline of the measured resistance due to the current is less than 0.1%.
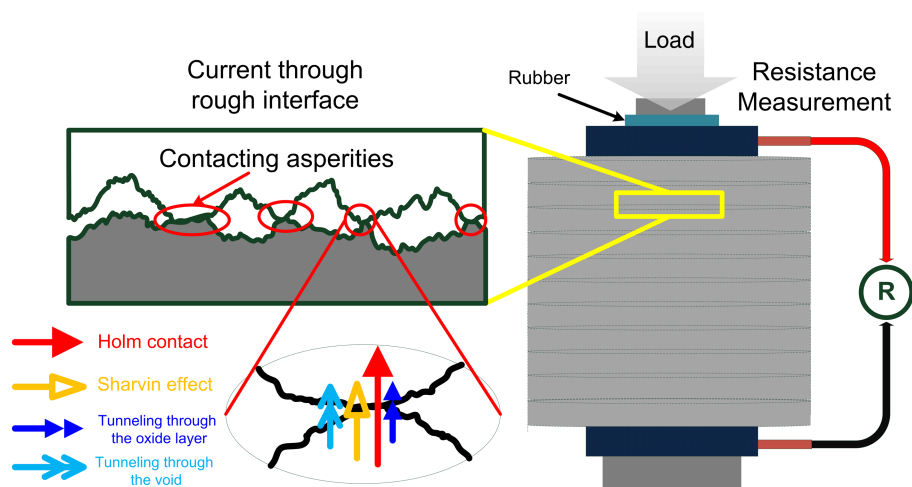

Fig. 2. Experimental setup for the resistance measurement of a stack of rough surfaces and schematic of the current flow through rough interfaces by means of Holm contact, Sharvin contact and quantum tunneling
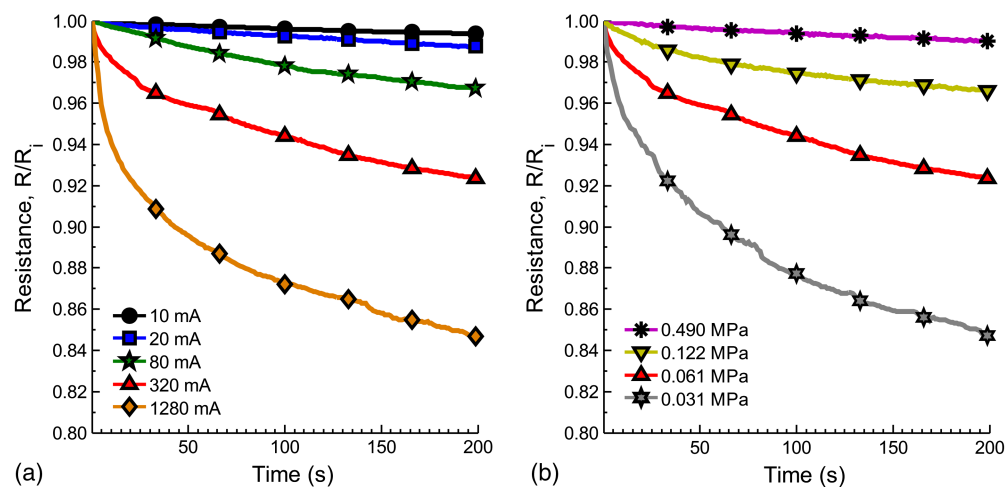
Fig. 3. Typical resistance relaxation curves over 200 s, with R_i being the initial measured resistance: (a) with constant applied stress being 0.061 MPa under various testing current (10, 20, 80, 320, and 1,280 mA with the initial resistance being 1.57, 1.46, 0.93, 0.76, and 0.23 Ω, respectively); (b) with the constant testing current being 320 mA under various compressions (0.031, 0.061, 0.122, and 0.490 MPa with the initial resistance of 2.01, 0.76, 0.59, and 0.18 Ω, respectively)

Sweeping Current Tests

The influence of the testing current on measured ECR was assessed by sweeping current tests. Here the applied sweep current test consisted of two phases with the *loading* phase (P1) having a logarithmically increasing current from 0.0001 to 1.5 A and the *unloading* phase (P2) having a logarithmically decreasing current from 1.5 A back to 0.0001 A. During the sweep procedure, the voltage was recorded at a data acquisition frequency of 2 kHz corresponding to the electrical current imposed. The normal pressure applied on the measured samples was 30 N, corresponding to a stress level of 0.061 MPa. The sweep process, including both phases, was accomplished within 0.2 s in order to avoid the occurrence of electrical degradation over time. As discussed in the previous section, when the conduction time is shorter than 1 s, the time-dependant reduction in resistance is negligible. Figs. 4(a and b) show the measured voltage and contact resistance with respect to testing current for the three types of samples. The shape of voltage hysteresis loops

is seen to be consistent for the three surface types while presenting different voltage levels. In Fig. 4(b), the measured results of all three surfaces demonstrate similar trends known as the Branly effect (Castaing and Laroche 2004; Falcon and Castaing 2005), i.e., the measured resistance begins to drop after the testing current reaches a certain value, after which the resistance appear to be irreversible as the current sweeps back. The corresponding threshold current values for S1, S2, and S3 are around 150, 80, and 60 mA, respectively, and the values seem to inversely correlate with the fractal dimension of the surface. However, the definite correlation between the RMS roughness and the threshold current can only be concluded by extending the types of surfaces. The use of RMS roughness is limited in predicting interface behaviors, whereas the fractal dimension, a cross-scale descriptor, is extensively used to interpret surface phenomena, such as conduction properties at rough interfaces (Kogut and Komvopoulos 2005; Persson 2006). The transition at the threshold current may come from the electrothermal coupling of the microcontacts at rough interfaces.
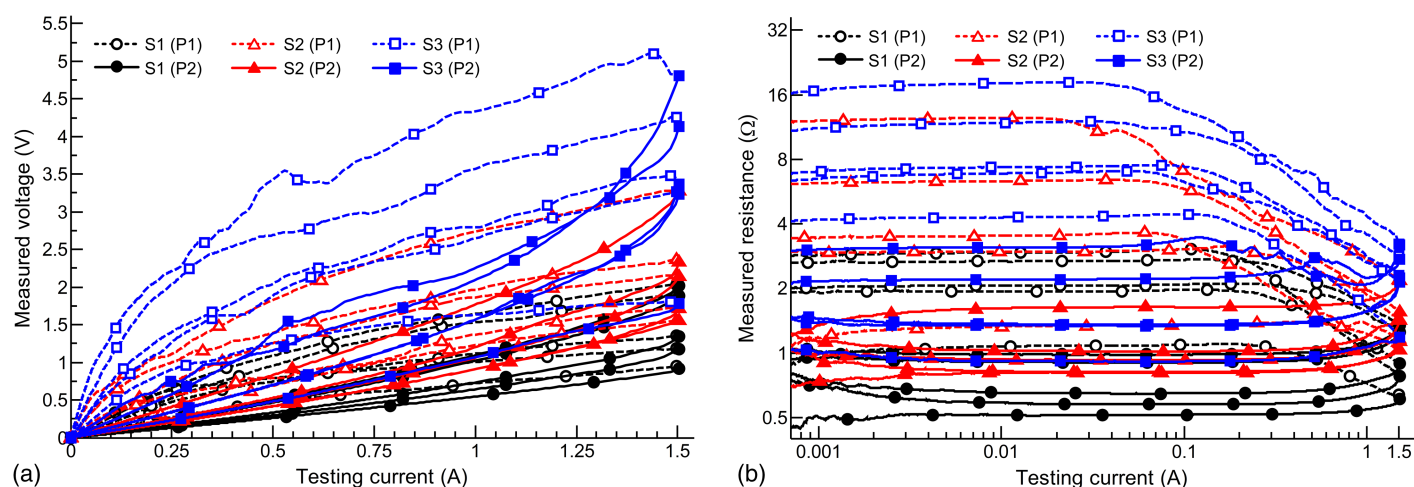

Fig. 4. Typical measured results for three types of samples using sweeping currents under a constant stress of 0.061 MPa; the data presented by the solid lines describes the first phases with increasing testing currents and the dashed lines show the second phases with decreasing currents: (a) variation of the measured voltage; (b) resistance-current characteristics

For testing currents higher than approximately 5 mA and lower than the threshold current values, the measured resistances remain stable on two plateaus in both P1 and P2, with a larger value obtained for P1, shown in Fig. 4(b). In other words, ohmic behavior at low levels of electrical current was found for all three types of surfaces. As shown in Fig. 4(b), at low testing currents (lower than 1 mA) in either P1 or P2, the measured resistances exhibit instability, especially for polished samples. Measurement noise for all three surfaces is observed at similar levels, which are amplified in logarithmic scale, being prominent when the measured resistances are small.

For each type of surfaces, the range of measured voltage and resistance was found to vary in five different tests under the same experimental conditions, e.g., the measured resistance of polished samples spreads from 0.5 to 3 Ω. From the experimental results, the surfaces described by higher fractal dimension demonstrate larger values of measured resistances. Specifically, the smallest resistances are observed from polished samples and the largest resistances are measured from the samples blasted using glass beads of 50 μm diameter. The polished samples present the smoothest and the most stable trends among the three types of surfaces. High level noises are found for surfaces after sand blasting procedures showing more complex topographies, which may cause the sensitivity to the microvibration from the loading device and the electrical noise from the measurement unit.

By rearranging the sample stacking order or by rotating the samples to achieve different contact configurations one can retrieve the voltage hysteresis loops and repeat the processes depicted in Fig. 4. Despite this, all the samples used were repolished and sand blasted again between successive tests to avoid the accumulation of surface modification by current flow as the sweep procedure may bring about some localized modification of the surface characteristics or possible changes of surface chemical composition.

A further test was done by driving successive back-and-forth scanning current cycles with increasing current range. A typical obtained result for polished samples is shown in Fig. 5. Here each successive current cycle was of 0.2 s duration and compressive pressure was maintained at 0.02 MPa during all nine sweep cycles. The sweeping current range was increased by a factor of $\sqrt{2}$ at each consecutive cycle until the current sweep reached 1.5 A. There exists a pause of around 10 s for data exporting and setting of the source/measurement unit. Additionally, tests with a longer pause up to several minutes were conducted and presented the same trends. For all nine cycles, the electrical current flows at different levels can modify the ECR of interfaces at different degrees. At each individual cycle, the measured voltages and resistances tend to be reversible when the testing current is lower than the maximum current of the previous cycle, i.e., the measured voltages and resistances in P1 branch are inversely along the track of P2 of the previous cycle, exhibiting ohmic conduction properties. The envelope line constituted by P1 of the first cycle, P2 of the last cycle, and the resistance declining segments in P1 of all nine cycles, exhibits a similar curve shapes as that of each individual cycle. The threshold current values at the turning point for measured resistance in all cycles grow from around 100 mA to 1 A, along with the increasing range of the imposed sweeping current.

Even though all the tests were performed over a short duration, i.e., 0.2 s, the Joule heating generated from the testing current may still have an effect on the measured resistance. In Fig. 5(b), evident upward and downward trends are observed at the end of P1 and at the beginning of P2, respectively. The aluminium has a lower heat capacity than the oxide. The Joule heating is likely to contribute to the trends to a certain extent. The irreversible Joule heating from the injected current, which accumulates with respect to time, cannot fully explain the reversible upward and downward trends at the end of P1 and the beginning of P2. Another possible reason can be the charging and discharging processes occurring during the tests. The contact of rough interfaces can be regarded as a complex network of resistors and capacitors that vary with the applied pressure and injected current. Moreover, this process is very similar to the conduction behaviors in semiconducting devices showing nonlinear and reversible properties.

A further experimental study was conducted in order to shed light on relations between the applied load and ECR. For polished surfaces, five typical voltage-current loops and resistance-current characteristics under various loads ranging from 0.031 to 0.490 MPa were obtained and are shown in Fig. 6. Under a high compressive pressure (more than 0.490 MPa), the loops become flat, i.e., P2 follows the same path as P1. The Branly effect tends to be harder to capture when the pressed surfaces were in contact at sufficiently high stress values. A high level of applied stress leads to better stability and repeatability of ECR measurements.
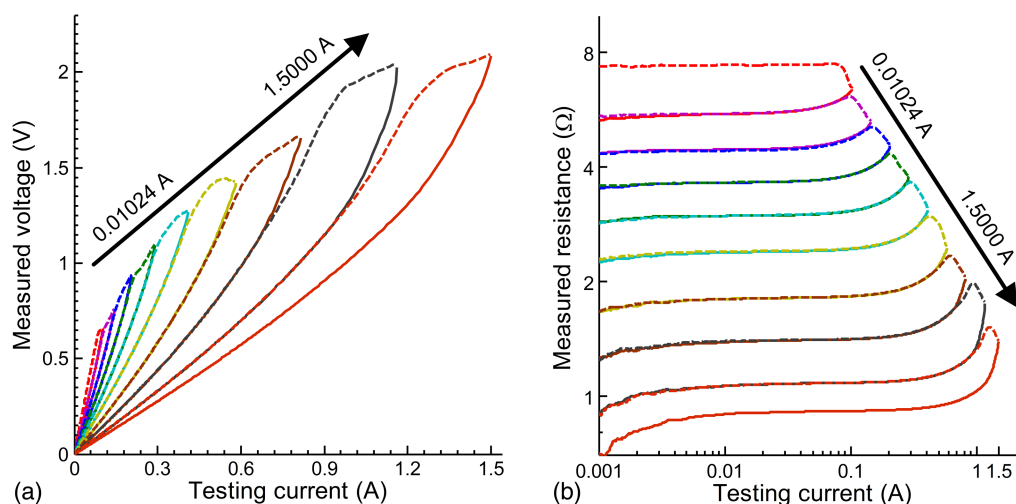

Fig. 5. Typical measured results for a stack of polished samples with nine successive back-and-forth sweeping current cycles with range increasing by a factor of $\sqrt{2}$ from 0.1024 to 1.5000 A (0.1024, 0.1448, 0.2048, 0.2896, 0.4096, 0.5793, 0.8192, 1.1585 and 1.5000 A) under a constant stress of 0.02 MPa: (a) hysteresis loops of voltage; (b) resistance-current characteristics
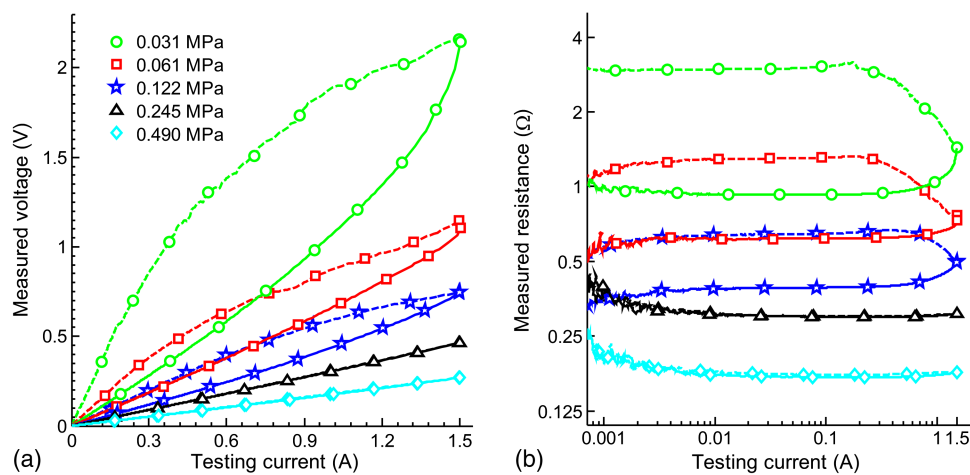
Fig. 6. Typical measured results for polished samples using current sweep under various stresses with solid lines expressing the first phase and the dashed line showing the second phase: (a) variation of the measured voltage; (b) resistance-current characteristics

The adjacent asperities may move closer to each other under a higher contact pressure, which results in the rise of the contacting area, thus enhances the conduction. The enlarged contacting area can carry more current without the microsoldering of the contact points. In engineering practice, the contact resistance is usually reduced by squeezing the contacting components together with greater force, which can bring about a larger true contact area. With the sweep tests shown here, the electrical current seems to be also capable of broadening the current path.

Stress-Dependent Electrical Contact Resistance

The results shown in Figs. 3–6 indicate a likely change of the contact network between the surfaces, where the contacting asperities can be regarded as a network of resistors and capacitors changing with applied current, mechanical load, and time. The true contact area increases linearly with the applied compression, resulting in improved conduction (Kogut 2005; Kogut and Komvopoulos 2005). Meanwhile, the electrical current results in the physical and chemical modification of sample surfaces, which involves many processes, including the rupture of the oxide layer due to compression and the localized heating induced by current.

With the tests presented above, the conclusions are (1) for the studied systems, when the imposed current is less than 50 mA, impact from the current on the measured resistance is negligible, even at low levels of applied stress (lower than 0.020 MPa). However, a small testing current of less than 1 mA can lead to a high-level of measurement noise; and (2) when the conduction time of electrical current (less than 50 mA) is less than 1 s, the influence of the current on resistance can be ignored, especially in cases of high pressures (higher than 0.5 MPa).

For samples exhibiting different surface morphologies, the electrical resistances were measured under various stresses, as shown in Fig. 7. For each type of sample, five series of tests were conducted and the resistances were evaluated at 16 different stress levels from 0.020 to 8.936 MPa. The testing current was set as 10 mA and the measured time was 0.01 s for each individual data point in order to minimize the influence of the testing current on the measurement.

As shown in Fig. 7, the measured resistances of disk stacks with different surface features decrease considerably as the compressive pressure is increased, converging to a value close to the bulk resistance of the material. For the identical loading stress level, samples blasted with 50 μm sized glass beads usually present the highest

resistance among all three types of samples. At low levels of applied stress (less than 0.5 MPa), the measured resistance is spread across a wider range. A few groups of the testing results were not included when jumps occur in the resistance measurement under constant or smoothly increasing loads. The unexpected vibration, electrical noise and some limitations of the experimental setting can contribute to the measurement uncertainty. By fitting the resistance/ pressure curves from 0.031 to 1.176 MPa it is observed that the measured contact resistance is a power function of the compressive stress at certain range of loading with the exponents being -0.816, -1.026, and -1.494, respectively, for polished surface (S1), blasted using 300 μm (S2), and 50 μm (S3) diameter glass beads. The absolute values of power exponents demonstrate an increasing trend with the rise of fractal dimension indicated in Table 1. When a loading force of 4,384 N is applied, corresponding to a stress level of 8.936 MPa, the measured resistance can be as small
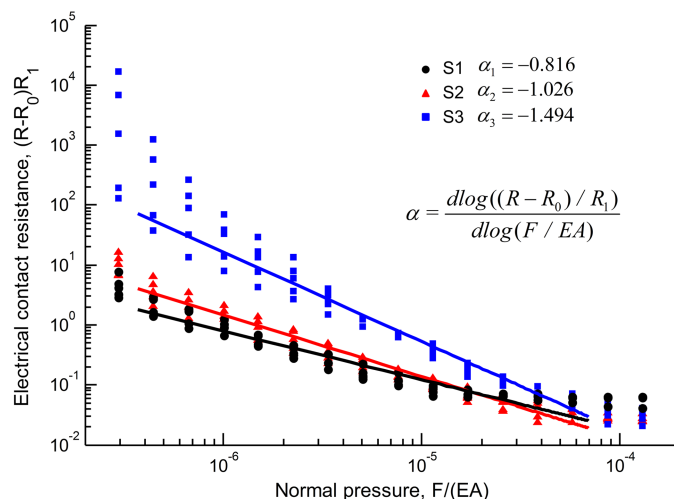

Fig. 7. Stress-dependent ECR of different surfaces under various loading levels with a testing current of 10 mA, with E being the value of the Young's modulus of the tested material, A being the projected area of the tested samples, R_0 being 0.06 Ω, including the combined resistance of bulk material of identical size as the disk stack (equaling 2.53 $\mu\Omega$), wires and connections used in the experimental setting, and R_1 being 1 Ω

as 0.0578, 0.0271, and 0.0303 Ω, corresponding to S1, S2, and S3. The resistance measured at high loads for the three types of tested surfaces appears to be inversely correlated with the values of RMS roughness and RMS slope. Further experiments with more types of surface are necessary to reach a general conclusion on the relationship between the stress-dependent electrical resistance and RMS roughness and RMS slope.

Conclusions

An experimental investigation was performed on the electrical contact resistance of rough surfaces. The experimental results show that the measured contact resistances of a stack of rough aluminium samples rely strongly on surface topology, mechanical loading, as well as testing current and time. The typical resistance creep curves over 200 s were recorded to investigate the current effect on the measured resistance over time. Tests with sweeping current under various compressive loads were carried out to study the influence of the current on the electrical contact resistance. For low-level electrical currents of the orders of a few mA, the electrical resistance is constant, exhibiting a linear ohmic behavior whereas the rise of the electrical current brings about a decrease of the electrical resistance. An increased compressive load results in the weakening of the effects of testing current on the measured resistance and decreases the time dependent resistance relaxation. Similarly, a higher testing current can also cause the reduction of the impact from the loading force. With testing current set as 10 mA and the measuring time being 0.01 s for each measured resistance, the impact of the current can be ignored for all three types of samples under varying loading levels. Under this condition, the measured resistances of stacks of samples decrease continuously under increasing stresses, approaching the resistance for bulk material at high loads. The results also demonstrate that a power law relationship exists between the measured electrical resistance and normal stress across a certain stress range, with the absolute values of exponents rising with the fractal dimension of the surfaces.

Acknowledgments

References

Agraıt, N., Yeyati, A. L., and Van Ruitenbeek, J. M. (2003). "Quantum properties of atomic-sized conductors." *Phys. Rep.*, 377(2), 81–279.

Archard, J. (1957). "Elastic deformation and the laws of friction." *Proc. R. Soc. London, Ser. A*, 243(1233), 190–205.

Barber, J. (2003). "Bounds on the electrical resistance between contacting elastic rough bodies." *Proc. R. Soc. London, Ser. A*, 459(2029), 53–66.

Bourbatache, K., Guessasma, M., Bellenger, E., Bourny, V., and Tekaya, A. (2012). "Discrete modelling of electrical transfer in multi-contact systems." *Granular Matter*, 14(1), 1–10.

Bowden, F., and Williamson, J. (1958). "Electrical conduction in solids. I: Influence of the passage of current on the contact between solids." *Proc. R. Soc. London, Ser. A*, 246(1244), 1–12.

Bryant, M. D. (1994). "Resistance buildup in electrical connectors due to fretting corrosion of rough surfaces." *Compon. Packag. Manuf. Technol. Part A IEEE Trans.*, 17(1), 86–95.

Bryant, M. D., and Jin, M. (1991). "Time-wise increases in contact resistance due to surface roughness and corrosion." *Compon. Hybrids Manuf. Technol. IEEE Trans.*, 14(1), 79–89.

Castaing, B., and Laroche, C. (2004). ""Turbulent" electrical transport in copper powders." *Europhys. Lett.*, 65(2), 186–192.

Chang, W., Etsion, I., and Bogy, D. B. (1987). "An elastic-plastic model for the contact of rough surfaces." *J. Tribol.*, 109(2), 257–263.

Ciavarella, M., Dibello, S., and Demelio, G. (2008). "Conductance of rough random profiles." *Int. J. Solids Struct.*, 45(3), 879–893.

Ciavarella, M., Murolo, G., and Demelio, G. (2004). "The electrical/thermal conductance of rough surfaces—the Weierstrass-Archard multiscale model." *Int. J. Solids Struct.*, 41(15), 4107–4120.

Creyssels, M., Dorbolo, S., Merlen, A., Laroche, C., Castaing, B., and Falcon, E. (2007). "Some aspects of electrical conduction in granular systems of various dimensions." *Eur. Phys. J. E Soft Matter Biol. Phys.*, 23(3), 255–264.

Creyssels, M., Falcon, E., and Castaing, B. (2009). "Experiment and theory of the electrical conductivity of a compressed granular metal." *Proc., 6th Int. Conf. on the Micromechanics of Granular Media*, American Institute of Physics, Melville, NY, 123–126.

Crinon, E., and Evans, J. (1998). "The effect of surface roughness, oxide film thickness and interfacial sliding on the electrical contact resistance of aluminium." *Mater. Sci. Eng. A*, 242(1), 121–128.

De Santis, A., Fedi, M., and Quarta, T. (1997). "A revisitation of the triangular prism surface area method for estimating the fractal dimension of fractal surfaces." *Ann. Geophys.*, 40(4), 811–821.

Dorbolo, S., Ausloos, M., and Vandewalle, N. (2002). "Hysteretic behavior in metallic granular matter." *Appl. Phys. Lett.*, 81(5), 936–938.

Dubuc, B., Zucker, S., Tricot, C., Quiniou, J., and Wehbi, D. (1989). "Evaluating the fractal dimension of surfaces." *Proc. R. Soc. London A. Math. Phys. Sci.*, 425(1868), 113–127.

Falcon, E., and Castaing, B. (1993). "Electrical properties of granular matter: From" Branly effect" to intermittency." *Proc., Geotechnical Management of Waste and Contamination*, CRC Press, London, U.K., 323.

Falcon, E., and Castaing, B. (2005). "Electrical conductivity in granular media and Branly's coherer: A simple experiment." *Am. J. Phys.*, 73(4), 302–307.

Falcon, E., Castaing, B., and Creyssels, M. (2004). "Nonlinear electrical conductivity in a 1D granular medium." *Eur. Phys. J. B*, 38(3), 475–483.

Foley, E., Candela, D., Martini, K., and Tuominen, M. (1999). "An undergraduate laboratory experiment on quantized conductance in nanocontacts." *Am. J. Phys.*, 67(5), 389–393.

Greenwood, J., and Williamson, J. (1958). "Electrical conduction in solids. II. Theory of temperature-dependent conductors." *Proc. R. Soc. London, Ser. A*, 246(1244), 13–31.

Hanaor, D., Gan, Y., and Einav, I. (2013). "Effects of surface structure deformation on static friction at fractal interfaces." *Géotechnique Lett.*, 3(2), 52–58.

Hanaor, D., Gan, Y., and Einav, I. (2015). "Contact mechanics of fractal surfaces by spline assisted discretisation." *Int. J. Solids Struct.*, 59, 121–131.

Holm, R., and Holm, E. A. (1967). *Electric contacts*, Springer, New York.

Jackson, R. L., Crandall, E. R., and Bozack, M. (2012). "An analysis of scale dependent and quantum effects on electrical contact resistance between rough surfaces." *Proc., Electrical Contacts (Holm), 2012 IEEE 58th Holm Conf. on*, IEEE, New York, 1–10.

Jackson, R. L., Malucci, R. D., Angadi, S., and Polchow, J. R. (2009). "A simplified model of multiscale electrical contact resistance and comparison to existing closed form models." *Proc., Electrical Contacts, 2009 Proc., 55th IEEE Holm Conf. on*, IEEE, New York, 28–35.

Kogut, L. (2005). "Electrical performance of contaminated rough surfaces in contact." *J. Appl. Phys.*, 97(10), 103723.

Kogut, L., and Etsion, I. (2000). "Electrical conductivity and friction force estimation in compliant electrical connectors." *Tribol. Trans.*, 43(4), 816–822.

Kogut, L., and Komvopoulos, K. (2003). "Electrical contact resistance theory for conductive rough surfaces." *J. Appl. Phys.*, 94(5), 3153–3162.

Kogut, L., and Komvopoulos, K. (2004). "Electrical contact resistance theory for conductive rough surfaces separated by a thin insulating film." *J. Appl. Phys.*, 95(2), 576–585.

Kogut, L., and Komvopoulos, K. (2005). "Analytical current-voltage relationships for electron tunneling across rough interfaces." *J. Appl. Phys.*, 97(7), 073701.

Meulenberg, W., Uhlenbruck, S., Wessel, E., Buchkremer, H., and Stöver, D. (2003). "Oxidation behaviour of ferrous alloys used as interconnecting material in solid oxide fuel cells." *J. Mater. Sci.*, 38(3), 507–513.

Mikrajuddin, A., Shi, F. G., Kim, H., and Okuyama, K. (1999). "Size-dependent electrical constriction resistance for contacts of arbitrary size: From Sharvin to Holm limits." *Mater. Sci. Semicond. Process.*, 2(4), 321–327.

Milanez, F. H., Yovanovich, M. M., and Culham, J. R. (2003). "Effect of surface asperity truncation on thermal contact conductance." *Compon. Packag. Technol. IEEE Trans.*, 26(1), 48–54.

Ogumi, Z., and Inaba, M. (1998). "Electrochemical Lithium Intercalation within carbonaceous materials: Intercalation processes, surface film formation, and lithium diffusion." *Bull. Chem. Soc. Japan*, 71(3), 521–534.

Oh, H.-J., Jang, K.-W., and Chi, C.-S. (1999). "Impedance characteristics of oxide layers on aluminium." *Bull. Korean Chem. Soc.*, 20(11), 1340–1344.

Paggi, M., and Barber, J. (2011). "Contact conductance of rough surfaces composed of modified RMD patches." *Int. J. Heat Mass Transf.*, 54(21), 4664–4672.

Persson, B. N. J. (2006). "Contact mechanics for randomly rough surfaces." *Surf. Sci. Rep.*, 61(4), 201–227.

Pohrt, R., and Popov, V. L. (2012). "Normal contact stiffness of elastic solids with fractal rough surfaces." *Phys. Rev. Lett.*, 108(10), 104301.

Pohrt, R., and Popov, V. L. (2013). "Contact stiffness of randomly rough surfaces." *Sci. Rep.*, 3, 3293.

Sharvin, Y. V. (1965). "On the possible method for studying Fermi surfaces." *Zh. Eksperim. i Teor. Fiz.*, 48, 984–985.

Slade, P. G. (2013). *Electrical contacts: Principles and applications*, CRC Press, London, U.K.

Sun, M. (2001). "Conductivity of conductive polymer for flip chip bonding and BGA socket." *Microelectron. J.*, 32(3), 197–203.

Sun, M., Pecht, M. G., Natishan, M. A. E., and Martens, R. I. (1999). "Lifetime resistance model of bare metal electrical contacts." *Adv. Packag. IEEE Trans.*, 22(1), 60–67.

Tekaya, A., Bouzerar, R., and Bourny, V. (2012). "Influence of surface topology on the electrical response of many bead assemblies." *AIP Adv.*, 2(3), 032108.

Yan, W., and Komvopoulos, K. (1998). "Contact analysis of elastic-plastic fractal surfaces." *J. Appl. Phys.*, 84(7), 3617–3624.

Yanson, A., Bollinger, G. R., Van den Brom, H., Agrait, N., and Van Ruitenbeek, J. (1998). "Formation and manipulation of a metallic wire of single gold atoms." *Nature*, 395(6704), 783–785.

Zahn, W., and Zösch, A. (1999). "The dependence of fractal dimension on measuring conditions of scanning probe microscopy." *Fresenius' J. Anal. Chem.*, 365(1–3), 168–172.